

Thermal decomposition of lignocellulosic materials: comparison of the results obtained in different experimental systems

Rafael Bilbao, María Benita Murillo, Angela Millera
and José Francisco Mastral

*Department of Chemical and Environmental Engineering, Faculty of Science,
University of Zaragoza, 50009-Zaragoza (Spain)*

(Received 27 February 1991)

Abstract

An experimental system that allows the use of large particle sizes and the simulation of different operating conditions was built to study the thermal decomposition of lignocellulosic materials. The values of solid conversion and of temperature obtained at different points using spherical particles of pine wood 2 cm in diameter are shown. The conversion values are compared with those calculated from the equations obtained in a thermobalance for small particle sizes.

INTRODUCTION

A knowledge of the weight loss versus time in the thermal decomposition of lignocellulosic materials is important for the design and optimisation of different reactors (moving bed, rotatory furnace, . . .) used in gasification and pyrolysis processes.

In previous papers [1–5] a study of the thermal decomposition of different materials carried out in a thermobalance in a nitrogen environment was shown. Using small particle sizes, the behaviour of cellulose [1,2], xylan and lignin [3], “Pinaster” pine and barley straw [4] was analysed. In the same way, the relation between the results obtained from isothermal and dynamic experiments was determined [5].

It was concluded from these studies that the thermal decomposition of lignocellulosic materials is a complex process because of the different behaviour of each of the components which make up the material. Therefore, the kinetic equations are limited to specific conversion and temperature ranges.

To obtain the solid conversion with these equations, the solid temperature must be used, which may be different from the system temperature. Because

of this, a model which allowed the calculation of the relation between these temperatures was developed in the thermobalance study [2].

The application of this model to other experimental systems involves obtaining parameters which depend on experimental conditions. Furthermore, in the event of large particle sizes being used, temperature profiles in the solid may be produced. These profiles must be taken into account.

Therefore, an experimental system which allows the use of large particle sizes and the simulation of different operating conditions was built. In this work, the conversion and temperature results obtained with spherical particles of pine wood 2 cm in diameter are shown. The conversion values are compared with those calculated from the equations obtained in a thermobalance for small sizes.

EXPERIMENTAL METHOD

An illustration of the experimental system is shown in Fig. 1. It consists of a discontinuous cylindrical reactor for the solid, an electrical furnace connected to a temperature and heating rate control system and a data logger which allows the linking of ten thermocouples. Several of the thermocouples are placed inside the solid particle in order to ascertain the inner temperature profiles during the reaction. This experimental device allows the measurement of the weight loss of the solid during its thermal decomposition through a precision balance connected to the sample inside the reactor.

Experiments from 30–650 °C for different heating rates, β , of the system have been performed. Once 650 °C is reached, the system remains at this temperature for 12 minutes. A nitrogen flow rate of 15 cm³ s⁻¹ was used.

Experiments with wood spheres of different diameter (up to 5.65 cm) have been carried out. In this work, the results corresponding to a diameter of 2 cm ($W_0 = 2.5$ g) are shown. With this size, the error in the determination of weight loss is small and, in addition, the temperature at several points of the solid surface is similar and the inner temperature profiles of the solid are not very pronounced.

EXPERIMENTAL RESULTS

The main results obtained in four experiments carried out with different heating rates are shown in Tables 1–4.

The solid conversion has been determined on a dry basis, and the temperatures which are shown correspond to those of the system (T_1), the surface of the solid, $r/R = 1$ (T_2), $r/R = 0.83$ (T_3), $r/R = 0.47$ (T_4) and in the centre of the solid, $r/R = 0$ (T_5). It must be stressed that only a few representative results are shown, as temperature and weight loss data are recorded every 30 s and 5 s respectively.

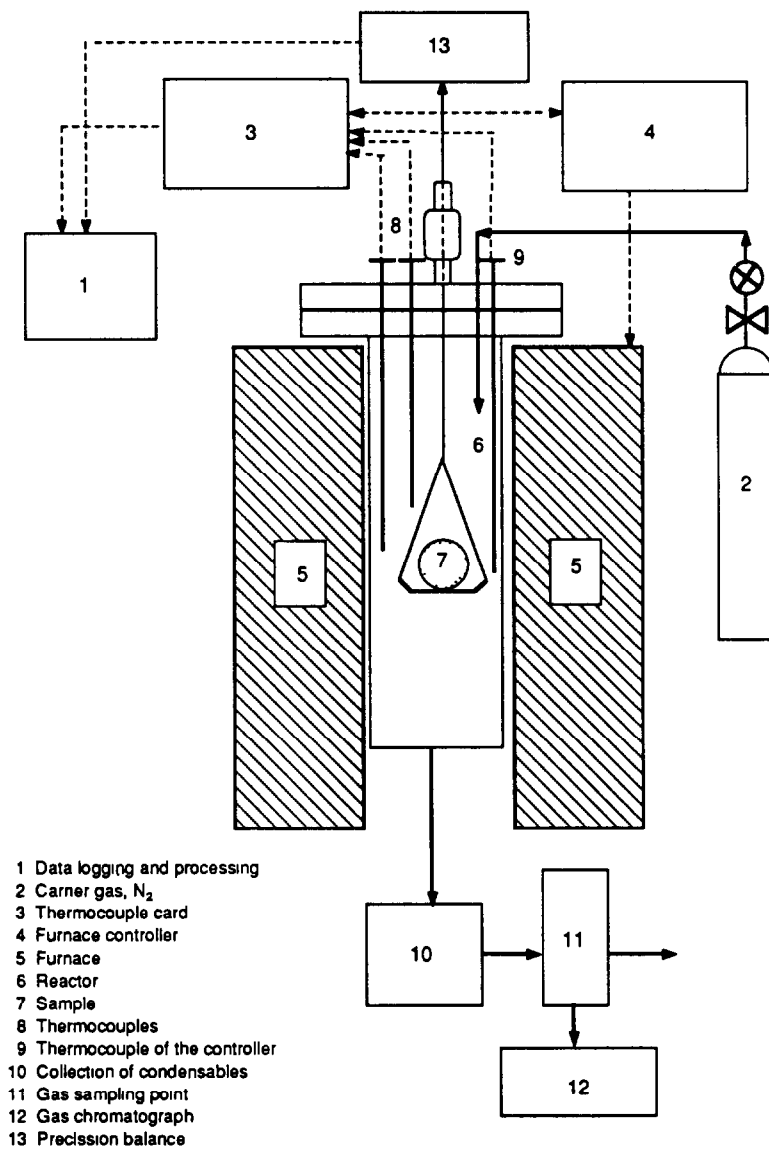


Fig 1. Experimental system.

As can be noted, the temperature differences between the system and the various inner points of the solid are marked. Moreover, it is observed that these differences become greater as the heating rate increases.

This trend is the same as that shown in previous papers involving studies with a thermobalance [5]. However, the differences between the system and solid temperatures, obtained for a certain heating rate, are very different. An example is shown in Fig. 2. This represents the temperature difference between the system and the solid surface just at the moment in which the thermal decomposition of the solid sample becomes noticeable. This point

TABLE 1

Results obtained for $\beta = 2^\circ \text{C min}^{-1}$

t (min)	T_1 ($^\circ\text{C}$)	T_2 ($^\circ\text{C}$)	T_3 ($^\circ\text{C}$)	T_4 ($^\circ\text{C}$)	T_5 ($^\circ\text{C}$)	X_s
0.00	31.6	25.6	22.6	23.0	25.3	0.000
15.09	80.4	63.0	54.8	55.7	61.7	0.000
30.18	92.2	70.9	60.3	61.6	70.1	0.000
45.27	110.6	93.8	88.2	88.8	94.4	0.000
60.36	140.4	123.8	125.8	124.4	125.8	0.028
75.45	170.1	150.6	156.6	153.5	155.1	0.035
90.54	199.9	181.0	187.7	179.3	182.7	0.048
105.63	239.6	215.1	213.5	210.3	218.0	0.052
120.72	283.0	259.1	258.1	253.7	265.8	0.070
135.81	302.8	282.4	290.0	283.7	286.3	0.109
150.90	326.8	306.9	306.6	300.5	306.1	0.178
155.93	347.7	331.2	326.9	320.6	330.3	0.231
160.96	345.8	332.6	330.0	322.2	333.2	0.268
165.99	370.0	353.5	345.0	338.5	349.9	0.342
171.00	363.3	346.3	345.4	337.6	344.2	0.444
176.03	388.8	366.6	358.0	352.3	364.9	0.516
181.06	384.3	370.6	368.0	359.5	366.8	0.574
196.15	421.7	405.7	394.4	388.2	394.4	0.612
211.24	453.2	432.8	433.1	425.0	435.4	0.694
226.33	474.3	459.8	449.5	442.4	454.8	0.698
241.42	514.5	503.7	486.2	478.9	496.6	0.701
256.52	542.0	531.7	519.5	511.6	525.9	0.780
271.62	561.3	550.4	538.7	529.7	542.5	0.792
286.73	596.3	580.9	575.5	567.3	579.5	0.802
301.84	625.2	615.2	601.4	593.2	609.4	0.813
306.89	635.9	621.7	612.3	604.8	619.0	0.815
315.91	650.4	636.2	627.1	619.1	634.0	0.816

has been selected for greater simplicity, since at that time there is no influence as yet of the heat of reaction of the thermal decomposition of the material. It can be observed that the differences of temperature are very disparate, being greater in the new system. This is due to the fact that the values of the parameters of the model [2] are different in the two cases, since they depend on variables such as the inert gas flow rate (which influences the individual heat transfer coefficient and the gas temperature), the size and weight of the solid, and even the position of the thermocouple. It must be stressed that it is necessary to calculate those parameters in each case, in order to use the model correctly.

Regarding the temperature difference between the system and the solid surface during thermal decomposition of the material, a trend similar to that obtained in the thermobalance is observed. In Fig. 3, the results from $\beta = 12.2^\circ \text{C min}^{-1}$ are shown. It can be noted that the difference in the temperatures decreases during the course of sample decomposition until a

TABLE 2

Results obtained for $\beta = 4.8^\circ\text{C min}^{-1}$

t (min)	T_1 ($^\circ\text{C}$)	T_2 ($^\circ\text{C}$)	T_3 ($^\circ\text{C}$)	T_4 ($^\circ\text{C}$)	T_5 ($^\circ\text{C}$)	X_s
0.00	33.1	24.4	23.2	18.0	16.1	0.000
8.04	73.4	54.6	53.6	46.8	42.3	0.000
16.08	123.0	89.3	87.9	76.1	65.3	0.000
22.11	142.5	109.9	109.5	101.2	86.4	0.014
30.15	194.2	156.1	156.1	148.4	125.7	0.021
36.18	205.7	185.5	177.0	183.1	176.4	0.120
42.21	251.0	224.6	219.7	218.5	209.5	0.121
48.24	263.5	248.7	238.9	247.0	245.4	0.145
54.27	311.0	288.8	280.2	286.8	277.1	0.234
60.30	322.3	311.8	298.8	309.5	316.5	0.258
62.31	333.9	317.4	304.0	315.2	316.4	0.313
64.32	351.7	332.6	323.6	331.1	323.9	0.386
66.33	371.1	351.3	344.6	349.0	340.3	0.470
70.35	376.8	366.6	349.3	367.8	372.5	0.491
72.36	381.3	366.9	353.3	366.2	366.8	0.545
74.37	394.5	375.9	364.4	374.4	370.2	0.607
79.38	434.3	419.5	402.8	420.1	420.9	0.670
82.41	432.2	418.3	403.8	413.5	423.7	0.771
88.44	471.2	450.2	439.4	446.3	443.7	0.790
94.47	491.0	473.7	459.2	472.6	471.8	0.812
100.45	520.7	507.5	497.2	506.7	505.6	0.820
106.44	547.5	532.9	523.6	530.5	530.1	0.820
112.46	574.2	557.7	548.9	553.5	554.1	0.820
118.45	600.5	581.3	572.8	574.4	577.7	0.820
124.44	626.6	603.9	595.1	593.2	600.6	0.820
130.44	650.3	626.8	617.9	615.6	621.8	0.820

conversion value of 0.2 is reached. The explanation of this lies in the increase of the solid temperature owing to the prevalence of the thermal decomposition of hemicelluloses, which is exothermic. At higher conversion, the cellulose decomposition (endothermic) and, subsequently, that of the lignin (exothermic) becomes significant.

COMPARISON WITH THE CALCULATED CONVERSIONS

The weight loss, on a dry basis, versus time corresponding to these experiments has been calculated from the equations obtained previously in studies with a thermobalance [5].

$$(dX_s/dt)_\beta = 0.0 \quad T \leq 162^\circ\text{C} \quad (1)$$

$$(dX_s/dt)_\beta = k_{s15}(A_s - X_s) + 0.0017(\beta - 1.5) \quad 162^\circ\text{C} < T \leq 290^\circ\text{C} \quad (2)$$

$$(dX_s/dt)_\beta = k_{s15}(A_s - X_s) + 0.0043(\beta - 1.5) \quad T > 290^\circ\text{C} \quad (3)$$

TABLE 3

Results obtained for $\beta = 7.8^\circ \text{C min}^{-1}$

t (min)	T_1 ($^\circ\text{C}$)	T_2 ($^\circ\text{C}$)	T_3 ($^\circ\text{C}$)	T_4 ($^\circ\text{C}$)	T_5 ($^\circ\text{C}$)	X_S
0 00	31 1	24.8	23 8	21.8	20 3	0.000
6.03	85.1	54.9	51 3	43.3	38.0	0.000
10.05	111.3	76.0	72.0	62.9	57.2	0.000
14 07	134 1	94.2	89.5	77.5	70.7	0 000
18.09	181.8	128.3	122.4	103 1	90.3	0.009
22 11	205 8	156.7	152.6	138.0	122.5	0.022
26.13	221 1	178 6	173.3	166.3	161.7	0.036
30 15	266.8	219.2	213 0	208 6	206.6	0.053
34 17	296.5	255 7	251 0	250.3	253 0	0.080
38.19	315.0	281.6	271 8	274 5	282.3	0.126
42 21	323.9	322.6	312.7	312.1	318 3	0 182
43.21	329.4	324 1	324.6	332.3	367.6	0.239
44 22	339 9	335 1	335.3	342.5	380.2	0 324
45 23	348.5	344.4	345 6	353.2	390 2	0.384
46.23	396.0	363.4	354.7	352.6	358.7	0.414
50 25	409 3	367 0	367.1	368.0	380 3	0 591
54.27	447 8	404.5	402 0	405 2	416.8	0 606
58.29	484.8	443.8	444.0	444 0	454.4	0 690
62 31	519 6	478.3	475.5	474.2	482 6	0 712
66.33	550 5	510 5	509 9	503.8	513.8	0.738
70.35	577 2	538 0	533.8	532 3	542.2	0.789
74 37	594 9	554 7	559.5	551.2	566 9	0 869
78 39	620 4	586.0	580.4	579.5	588 1	0.870
82 41	637 7	600.9	600.7	595 8	606.0	0.868
86 43	652 1	614 3	616 4	612.5	622 0	0 868

The kinetic coefficients (min^{-1}) are

$$k_{\text{SI}5} = 0.017 \quad T \leq 290^\circ \text{C} \quad (4)$$

$$k_{\text{SI}5} = 3.61 \times 10^4 \exp(-16400/RT) \quad 290^\circ \text{C} < T \leq 325^\circ \text{C} \quad (5)$$

$$k_{\text{SI}5} = 9.96 \times 10^{17} \exp(-52900/RT) \quad T > 325^\circ \text{C} \quad (6)$$

The values of A_S , the pyrolysable weight fraction, are shown in Fig. 4. The X_S values corresponding to each time have been calculated using the fourth order Runge-Kutta method.

First of all, these equations were solved using the system temperature T_1 . A comparison between the experimental and calculated results for different heating rates is shown in Figs. 5 and 6. It can be observed that the calculated values are always higher than the experimental ones and this difference increases as the heating rate increases. This can be due to the difference of temperatures existing between the system and the solid. For this reason, the equations have been solved again using the temperatures T_2 , T_3 , T_4 and T_5 shown in Tables 1-4.

TABLE 4

Results obtained for $\beta = 12.2^\circ \text{C min}^{-1}$

t (min)	T_1 ($^\circ \text{C}$)	T_2 ($^\circ \text{C}$)	T_3 ($^\circ \text{C}$)	T_4 ($^\circ \text{C}$)	T_5 ($^\circ \text{C}$)	X_s
0.00	28.1	22.5	20.9	20.2	19.3	0.000
4.02	59.7	42.3	40.5	33.6	30.7	0.000
8.04	112.4	77.4	70.8	60.6	55.5	0.000
12.06	180.0	126.5	122.2	96.6	86.3	0.000
16.08	247.9	191.0	188.8	155.5	131.2	0.042
18.09	282.6	232.8	230.8	204.6	187.7	0.129
20.10	313.7	269.4	270.0	252.6	248.3	0.063
22.11	345.4	314.7	309.4	300.5	303.3	0.161
24.12	376.1	349.5	346.9	341.9	351.1	0.240
25.12	388.0	362.5	352.6	351.5	360.1	0.362
26.13	403.4	374.6	393.2	363.2	369.7	0.482
27.13	417.1	389.8	414.8	381.7	393.5	0.651
28.14	430.2	411.1	413.4	403.0	419.0	0.660
32.16	474.5	454.3	450.2	445.4	456.6	0.719
36.18	513.7	487.7	497.7	478.7	488.0	0.822
40.20	547.9	521.7	525.4	511.4	523.4	0.776
44.22	574.3	552.7	565.6	541.8	551.1	0.782
48.24	600.6	582.5	585.8	568.2	578.5	0.803
52.26	621.6	606.8	615.3	590.3	601.1	0.812
56.28	640.5	627.5	622.4	610.6	622.2	0.809
60.30	654.5	640.6	637.3	640.6	636.7	0.812
64.32	636.1	625.8	627.7	606.9	621.1	0.819
68.34	642.5	634.4	626.9	613.2	625.0	0.818
71.36	650.6	642.3	632.8	620.1	631.0	0.820

Figures 7, 8, 9 and 10 show the comparison of the values of X_s vs. t obtained experimentally with those calculated from eqns. (1)–(6). It may be observed that the fitting can be considered satisfactory.

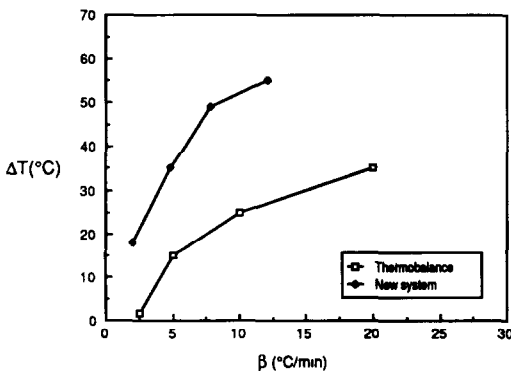


Fig. 2. Temperature differences in two experimental systems.

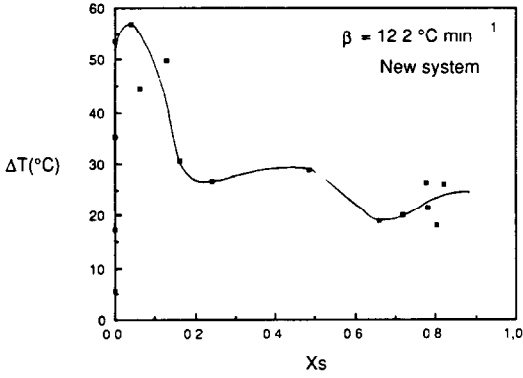


Fig. 3 Temperature difference between the system and the solid surface.

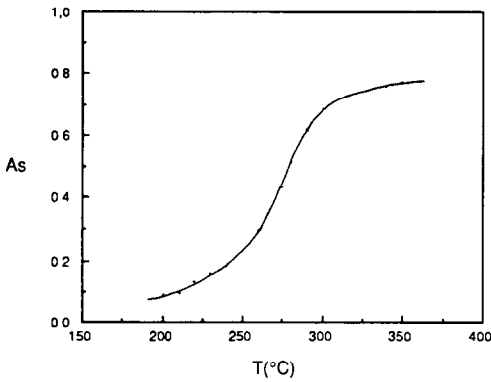


Fig 4 Pyrolysable weight fraction

Therefore, the main conclusions that can be obtained from this work are as follows.

(i) The application of the model developed for calculating the relation between the solid and system temperatures implies the previous determina-

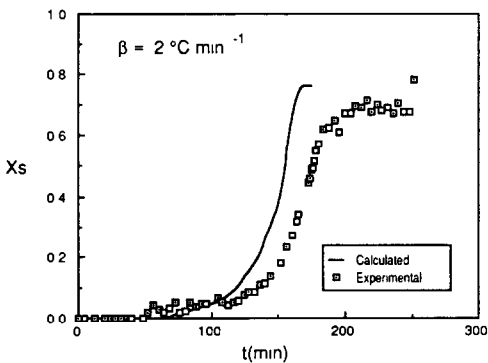


Fig 5 Comparison between the results using system temperature

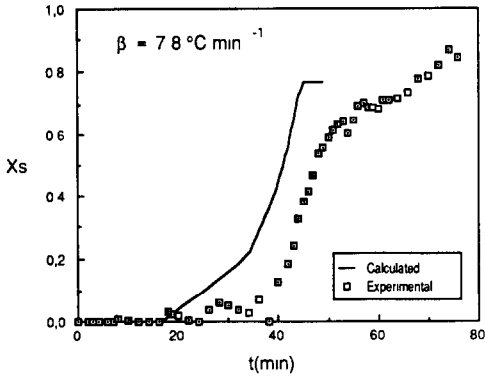


Fig. 6 Comparison between the results using system temperature

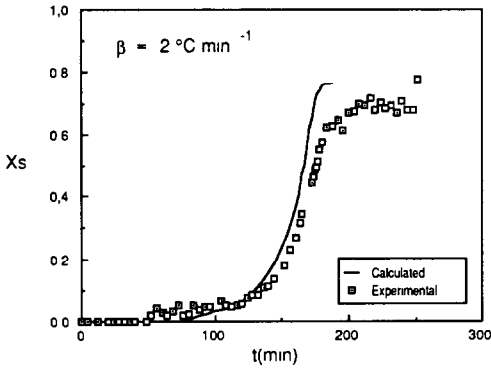


Fig. 7. Comparison between the results using solid temperature.

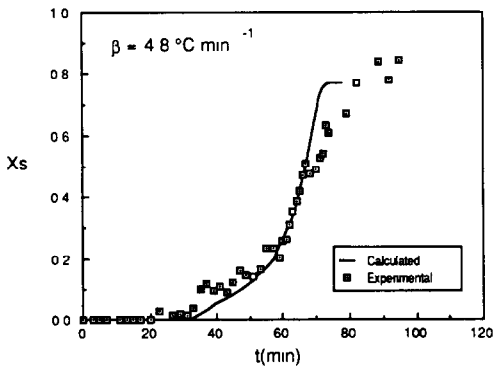


Fig 8. Comparison between the results using solid temperature.

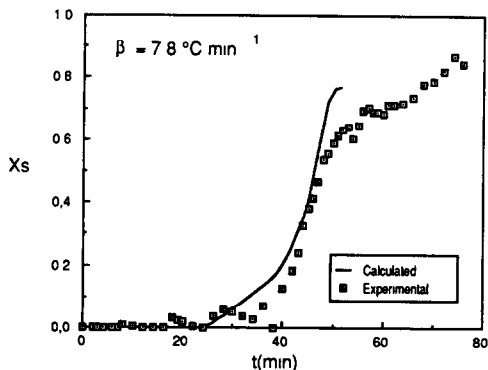


Fig. 9 Comparison between the results using solid temperature.

tion of its parameters, which depend on the experimental system and operating conditions.

(ii) The new experimental system is able to determine weight loss and temperature at several points in the solid sample, which may allow us to simulate the thermal decomposition of lignocellulosic materials under several operating conditions.

(iii) The equations obtained with the thermobalance to calculate weight loss in the thermal decomposition of lignocellulosic materials are applicable to other experimental systems whenever the true solid temperature is used.

ACKNOWLEDGEMENTS

The authors express their gratitude to DGICYT for providing financial support for this work (Project PB-88-0388) and also to Ministerio de Educación y Ciencia (Spain) for a research grant awarded to M.B.M.

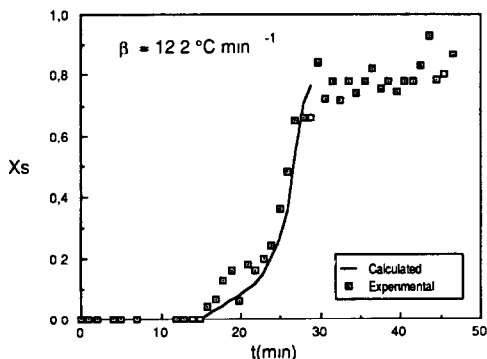


Fig. 10 Comparison between the results using solid temperature.

LIST OF SYMBOLS

A_S	pyrolysable weight fraction at a given temperature, dry basis
k_{S15}	kinetic coefficient for thermal decomposition of the solid, obtained from dynamic experiments at $\beta = 1.5^\circ \text{C min}^{-1}$
r	radius
R	radius of the solid particle
r/R	reduced radius
t	time
T	temperature
T_1	temperature of the system
T_2	temperature at the point $r = R$
T_3	temperature at the point $r/R = 0.83$
T_4	temperature at the point $r/R = 0.47$
T_5	temperature at the point $r/R = 0$
W_0	initial weight of solid
X_S	conversion of solid, dry basis
β	heating rate of the system

REFERENCES

- 1 R. Bilbao, J. Arauzo and A. Millera, *Thermochim. Acta*, 120 (1987) 121.
- 2 R. Bilbao, J. Arauzo and A. Millera, *Thermochim. Acta*, 120 (1987) 133.
- 3 R. Bilbao, A. Millera and J. Arauzo, *Thermochim. Acta*, 143 (1989) 137.
- 4 R. Bilbao, A. Millera and J. Arauzo, *Thermochim. Acta*, 143 (1989) 149.
- 5 R. Bilbao, A. Millera and J. Arauzo, *Thermochim. Acta*, 165 (1990) 103.